Nanostructures via Noncovalent Synthesis: 144 Hydrogen Bonds Bring Together 27 Components

Vasile Paraschiv,[†] Mercedes Crego-Calama,[†] Roel H. Fokkens,[†] Clemens J. Padberg,[‡] P. Timmerman,*[,†] and David N. Reinhoudt*[,†]

Laboratory of Supramolecular Chemistry and Technology and Materials Science and Technology of Polymers, MESA+ Research Institute, University of Twente, P.O. Box 217, 7500 AE Enschede, The Netherlands

d.n.reinhoudt@ct.utwente.nl

Received June 8, 2001

This paper describes the spontaneous and reversible assembly of ∼20 kDa synthetic hydrogen-bonded assemblies via the formation of 144 cooperative hydrogen bonds. These nanostructures (∼3.0 × 5.5 nm), consisting of 27 different components, have been carefully characterized using a combination of ^{1}H NMR spectroscopy, MALDI-TOF MS using Ag^+-labeling, gel permeation chromatography, and CD spectroscopy.

Introduction

Molecular recognition as a tool to assemble small organic molecules into predictable motifs has already proven its potential in the preparation of nanometer-scale structures with interesting optical or electronic properties.[1−3] This so-called bottom-up approach provides easy access to structures with 1−50 nm dimensions, a size regime that is perfectly compatible to that addressable via the classical top-down approach.[4] The spontaneous generation of well-organized supramolecular structures starts with a proper design of the molecular components. We have previously shown that calix[4]arenes serve as excellent molecular platforms for the prepositioning of melamine and/or cyanuric acid units, which are able to self-assemble into finite and infinite hydrogen-bonded complexes, both in solution[5] and on surfaces.[6] Currently, we are exploring the limits of the self-assembly approach by further increasing the complexity of the assemblies. In this paper, we describe our latest achievement in this study, that is the completely reversible formation of the nanostructures $\mathbf{1}_3$•$(DEB)_{24}$, $\mathbf{1}_3$•$(BuCYA)_{24}$, and $\mathbf{1}_3$•$(R\text{-}MePhCYA)_{24}$, comprising 8 different rosette layers that are held together by 144 cooperative hydrogen bonds. Regarding their size (∼3.0 × 5.5 nm) and molecular weight (∼20 kDa), these structures are comparable to small proteins, like cytochrome C (∼12 kDa) and myoglobin (∼16 kDa), or dendritic structures, like Zimmerman's self-assembled dendrimers (2.0 × 9.0 nm, ∼36 kDa) (Figure 1).[7]

Results and Discussion

Octamelamine **1** was prepared in one step from the mono-Boc-protected dimelamine carbamate **2a** and tetramelamine diamine **3a**. The reaction was performed by slow addition of **3a** (1.0 mM solution in CH_2Cl_2) to a solution of **2a** in CH_2Cl_2 in the presence of DIPEA (2.2 equiv) to give **1** in 31% yield after purification (Chart 1).

The 27-component hydrogen-bonded assembly $\mathbf{1}_3$•$(DEB)_{24}$ was prepared by simply mixing the octamelamine **1** with 8 equiv of 5,5-diethylbarbituric acid (DEB) in chloroform followed by sonication and heating at 50 °C overnight. Formation of the assembly is fully cooperative as judged from the fact that with only 4 equiv of DEB (half of the amount required for complete assembly formation) formation of intermediate assemblies was not observed at all. Addition of a slight excess (∼26.4 equiv) of *N*-butylcyanuric acid (BuCYA) or *N*-(1*R*-phenylethyl)-cyanuric acid (*R*-MePhCYA) to this assembly resulted in the quantitative replacement of the DEB units for the corresponding cyanurates, giving the new assemblies $\mathbf{1}_3$•$(BuCYA)_{24}$ and $\mathbf{1}_3$•$(R\text{-}MePhCYA)_{24}$ in quantitative yield. Characterization of the assemblies was performed using a combination of ^{1}H NMR spectroscopy, MALDI-TOF MS using Ag^+-labeling,[8] gel permeation chromatography,[9] and CD spectroscopy.[10]

The ^{1}H NMR spectrum of $\mathbf{1}_3$•$(DEB)_{24}$ in $CDCl_3$ clearly proves the successful formation of this octarosette assembly (Figure 2). The NH_{DEB} protons give rise to eight (partially overlapping) singlets between 12 and 15 ppm.

[†] Laboratory of Supramolecular Chemistry and Technology.
[‡] Materials Science and Technology of Polymers.

(1) Carter, F. L. *Molecular Electronic Devices II*; Marcel Dekker: New York, 1982.
(2) Murray, R. W. In *Chemical Sensors and Microinstrumentation*; Melchior, D. C., Bassett, R. L., Eds.; ACS Symposium Series 403; American Chemical Society: Washington DC, 1989; pp 1−19.
(3) Ajayan, P. M. *Chem. Rev.* **1999**, *99*, 1787−1799.
(4) Xia, Y.; Rogers, J. A.; Paul, K. E.; Whitesides, G. M. *Chem. Rev.* **1999**, *99*, 1823−1848.
(5) Timmerman, P.; Vreekamp, R. H.; Hulst, R.; Verboom, W.; Reinhoudt, D. N.; Rissanen, K.; Udachin, K. A.; Ripmeester, J. *Chem. Eur. J.* **1997**, *3*, 1823−1832.
(6) Klok, H.-A.; Jolliffe, K. A.; Schauer, C. L.; Prins, L. J.; Spatz, J. P.; Moller, M.; Timmerman, P.; Reinhoudt, D. N. *J. Am. Chem. Soc.* **1999**, *121*, 7154−7155.
(7) Zimmerman, S. C.; Zeng, F.; Reichert, D. E. C.; Kolotuchin, S. V. *Science* **1996**, *271*, 1095−1098.
(8) Timmerman, P.; Jolliffe, K. A.; Crego-Calama, M.; Weidmann, J.-L.; Prins, L. J.; Cardullo, F.; Snellink-Ruel, B. H. M.; Fokkens, R.; Nibbering, N. M. M.; Shinkai, S.; Reinhoudt, D. N. *Chem. Eur. J.* **2000**, *6*, 4104−4115.
(9) Mammen, M.; Simanek, E. E.; Whitesides, G. M. *J. Am. Chem. Soc.* **1996**, *118*, 12614−12623.
(10) Prins, L. J.; Huskens, J.; De Jong, F.; Timmerman, P.; Reinhoudt, D. N. *Nature (London)* **1999**, *398*, 498−502.

10.1021/jo0105742 CCC: $20.00
Published on Web 10/11/2001

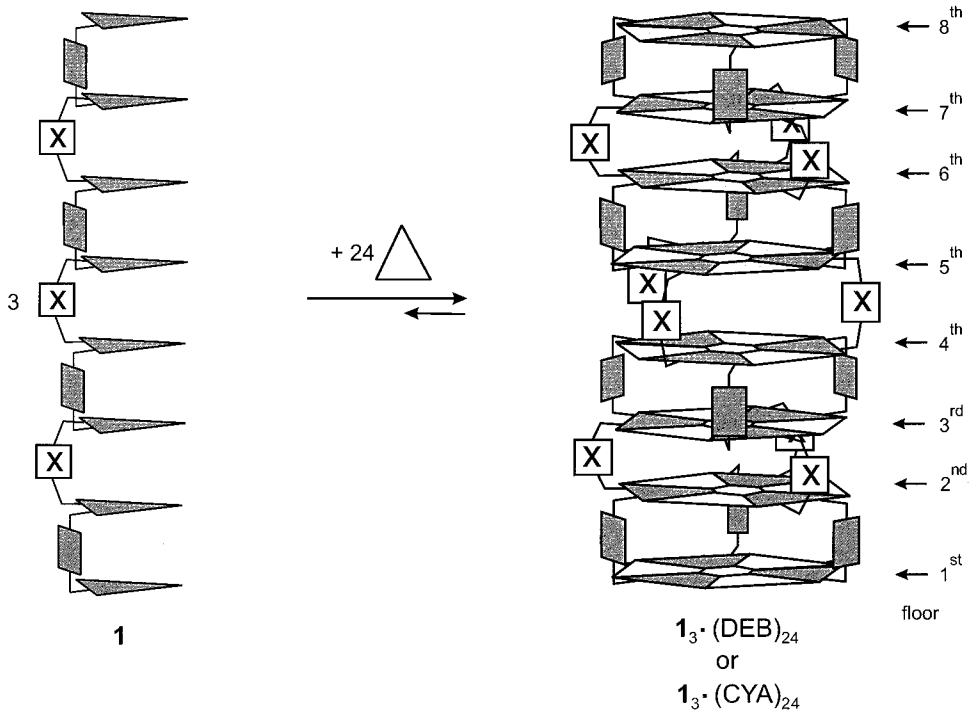

Figure 1. Schematic representation for self-assembly of the 27-component octarosette $\mathbf{1}_3$·$(DEB)_{24}$ and $\mathbf{1}_3$·$(CYA)_{24}$.

The signals for the top and bottom "floors" (first and eighth floors) are significantly different from the other resonances and are observed at 14.19 (H_a) and at 13.3 (H_b). The NH_{DEB} protons that are located at the inside of the assembly (second to seventh floors) are grouped around 13.8−13.6 (H_a, 9 H's) and 13.0−12.8 (H_b, 9 H's) ppm, characterizing the shielded environment of these protons. Additional proof for assembly formation comes from the four singlets between 8.6 and 8.2 (H_c) and the broad resonances around 7.7−7.4 ppm (H_d) for the other hydrogen-bonded NH protons. The ArH_h protons are clearly discernible, giving two sharp resonances around 6.0 ppm. Finally, a broad signal around 5.0 ppm is observed for the urea and carbamate NH protons. For the corresponding tetrarosette assembly $\mathbf{3b}_3$·$(DEB)_{12}$, the identity of all the proton signals was established using 2D NOE experiments.[11] The 1:8 stoichiometry of **1** and DEB was confirmed by careful integration of the NH_{DEB} and $ArCH_2Ar$ (4.5−4.2 ppm) proton signals.

The ^{1}H NMR spectrum for assembly $\mathbf{1}_3$·$(BuCYA)_{24}$ is severely broadened in comparison to that of $\mathbf{1}_3$·$(DEB)_{24}$, while the spectrum of assembly $\mathbf{1}_3$·$(R\text{-MePhCYA})_{24}$ is almost uninterpretable between 15−12 ppm. This is due to different orientations of the side chains of either BuCYA or *R*-MePhCYA, either up or down, within the octarosette assembly, which causes desymmetrization of the assembly. For BuCYA, exchange between the many different orientations is slow on the NMR time scale at room temperature, but becomes much faster at higher temperatures, which results in sharpening of the spectrum. The NH_{CYA} protons of assembly $\mathbf{1}_3$·$(BuCYA)_{24}$ are slightly shifted downfield to 14.65 (3 protons), 14.35 (9 protons), 14.12 (3 protons), 13.9 (9 protons) ppm. For this assembly the same 1:3:1:3 integral ratio of the various proton signals was observed, despite the much broader nature of the signals. Similarly, the other NH and ArH protons signals are observed in or around the same region as for assembly $\mathbf{1}_3$·$(DEB)_{24}$.

Characterization of assembly $\mathbf{1}_3$·$(EPB)_{24}$ (5-ethyl-phenyl barbituric acid) was also performed by MALDI-TOF mass spectrometry using a recently developed Ag^+-labeling technique.[8] Therefore, the assembly was treated with 1.5 equiv of $AgCF_3COO$ in $CHCl_3$ for 24 h prior to the measurement. The spectrum clearly confirms the presence of the rosette assemblies, showing a sharp and intense signal at m/z = 19 681 (calcd for $C_{1044}H_{1344}N_{234}O_{150}$·$^{107}Ag^+$ = 19 679.2) (see Figure 3). Additional signals were observed at m/z = 9851 ($[\mathbf{1}_3$·$(EPB)_{24} + Ag + Na]^{2+}$, calcd 9851.0), and 13 560, which is most likely due to clustering of free **1** with Ag^+. The shoulder (30% intensity) of the main peak at m/z = 19 902 arises from additional complexation of $AgCF_3COO$ ($[\mathbf{1}_3$·$(EPB)_{24} + 2Ag + CF_3COO]^+$, calcd 19 900.1) to one of the remaining 23 binding sites for Ag^+.

Additional proof for assembly formation was obtained using gel permeation chromatography (GPC), using monodisperse polystyrene as a reference. Earlier work by Whitesides clearly showed that the thermodynamic stability of the assemblies determines the shape of the peak.[9] The chromatogram of free **1** (not shown) indeed shows very broad peaks, most likely resulting from strong self-association of the monomer that leads to the formation of ill-defined polymeric structures. In contrast to this, the octarosette assembly $\mathbf{1}_3$·$(BuCYA)_{24}$ exhibits a sharp peak around 21 mL plus an additional peak for the liberated DEB (not shown). The peak for $\mathbf{1}_3$·$(BuCYA)_{24}$ is of comparable width and shape as that of the assemblies $\mathbf{2b}_3$·$(BuCYA)_6$, $\mathbf{3b}_3$·$(BuCYA)_{12}$, and $\mathbf{4}_3$·$(BuCYA)_{18}$ (Figure 4), thus confirming the monodisperse nature of the octarosette assembly. Moreover, dissociation of the assembly does not seem to occur on the GPC column.

Finally, we studied the formation of octarosette assemblies by CD spectroscopy. Like for most double and

(11) Kerckhoffs, J. K. M. A.; Crego-Calama, M.; Luyten, I.; Timmerman, P.; Reinhoudt, D. N. *Org. Lett.* **2000**, *2*, 4121−4124.

Chart 1

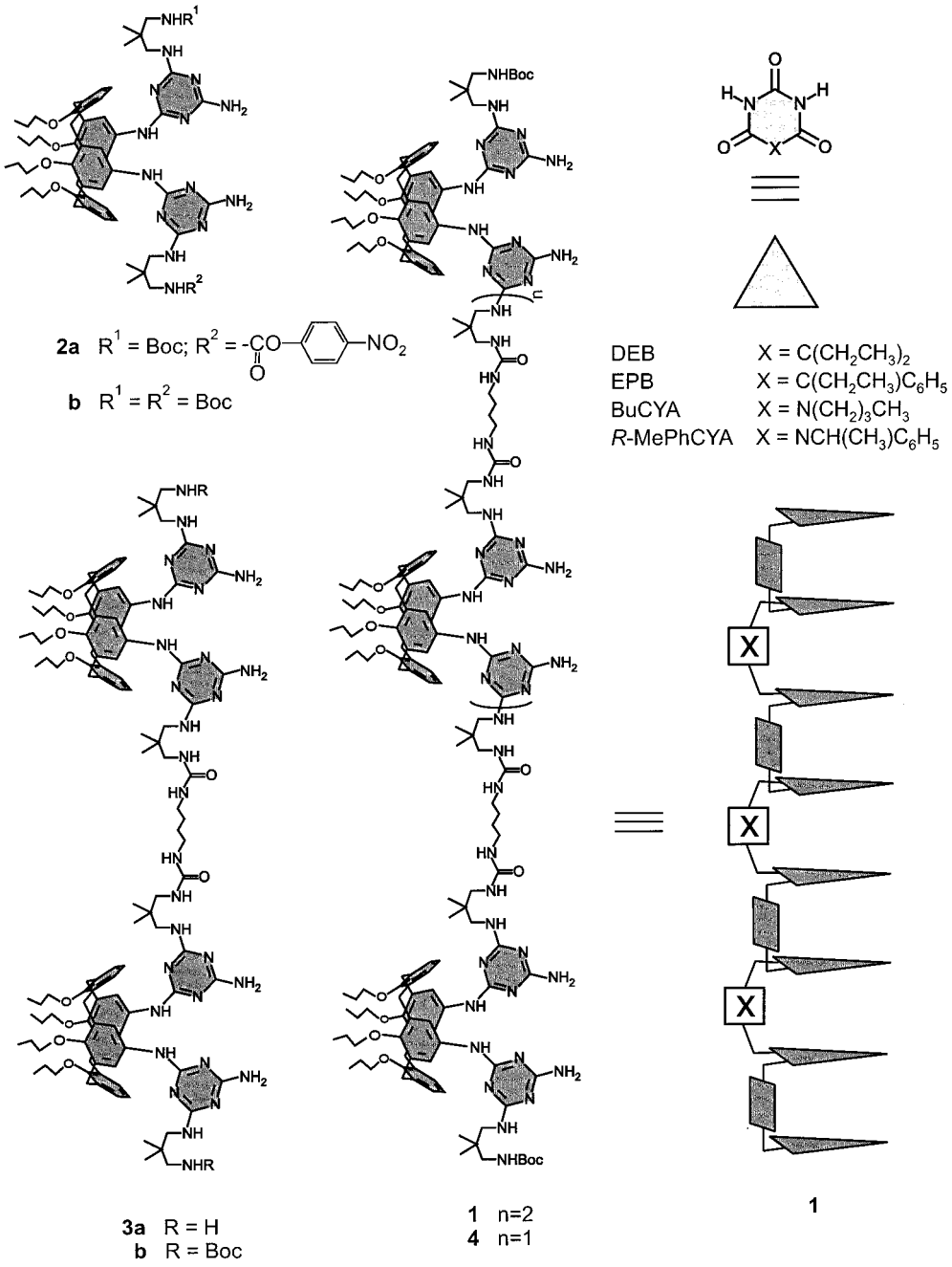

tetrarosette assemblies studied sofar, both octarosette assemblies $\mathbf{1}_3$·(DEB)$_{24}$ and $\mathbf{1}_3$·(BuCYA)$_{24}$ also display chirality at the supramolecular level, resulting from the dissymmetrical orientation of the components within the assembly.[6,12] When no chiral centers are present in the components, these assemblies are present as a racemic mixture of the *M*- and *P*-enantiomers. However, by using the chiral cyanurate *R*-MePhCYA, the corresponding assembly $\mathbf{1}_3$·(*R*-MePhCYA)$_{24}$ most likely forms exclusively the *M*-diastereomer, as was observed in very similar experiments with double rosette structures,[10] resulting from a quantitive induction of the chirality by the 24 chiral centers in the periphery. As a consequence, the assembly is strongly CD-active while no significant CD activity was observed for the individual components, which allows us to use CD spectroscopy for characterization. The CD-spectrum for $\mathbf{1}_3$·(*R*-MePhCYA)$_{24}$ (Figure 5) clearly proves the rosette-like structure of the assembly, since the spectrum very much resembles that of double rosette assembly $\mathbf{2b}_3$·(*R*-MePhCYA)$_6$. The intensity of the observed Cotton effect is somewhat lower than expected, i.e., roughly three times that of $\mathbf{2b}_3$·(*R*-MePhCYA)$_6$, indicating that the observed Cotton effects are not entirely additive.

To visualize the shape and structure of the octa rosette assembly, we performed computer simulation (Quanta/CHARMm 24.0, Figure 6). The structure was manually put together starting from the minimized structure obtained from NOE distance constraints measurements as described for assembly $\mathbf{2b}_3$·(DEB)$_6$.[11] The size of the octarosettes reaches 5.5 nm, comparable in size to the DNA oligomers used for conductivity measurements.[13]

(12) Paraschiv, V.; Crego-Calama, M.; Luyten, I.; Timmerman, P.; Reinhoudt, D. N. Manuscript in preparation.

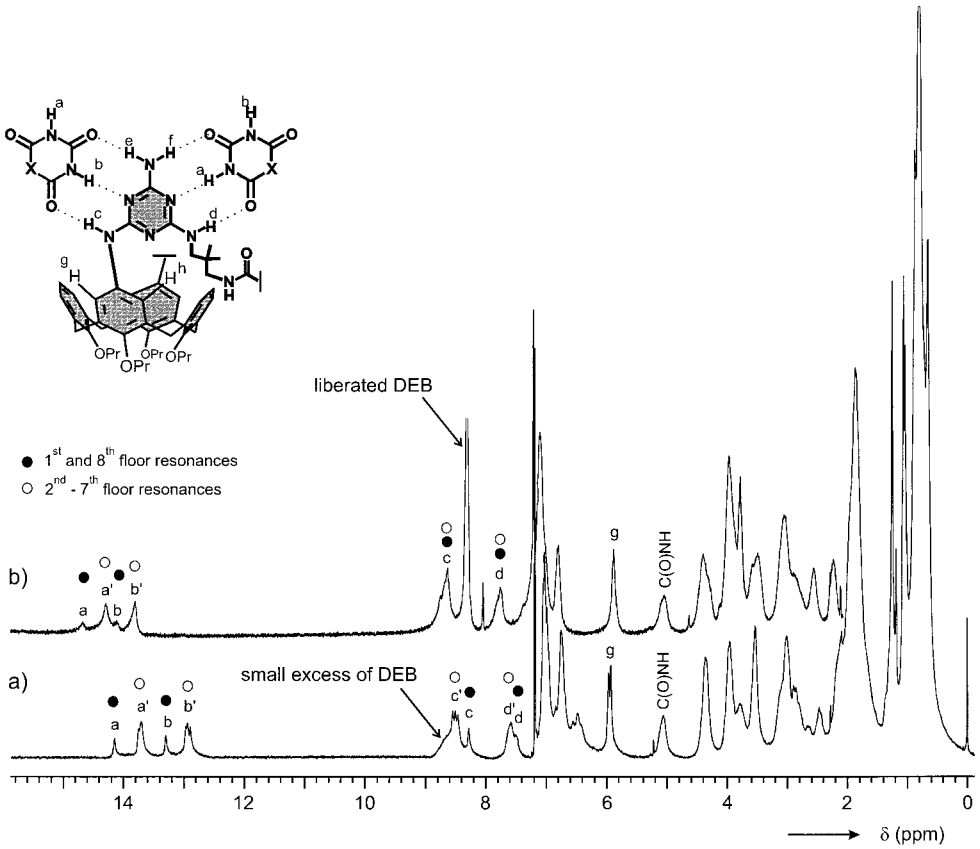

Figure 2. ^{1}H NMR spectra (300 MHz) of octarosette assemblies (a) $\mathbf{1}_3$·$(DEB)_{24}$ and (b) $\mathbf{1}_3$·$(BuCYA)_{24}$.

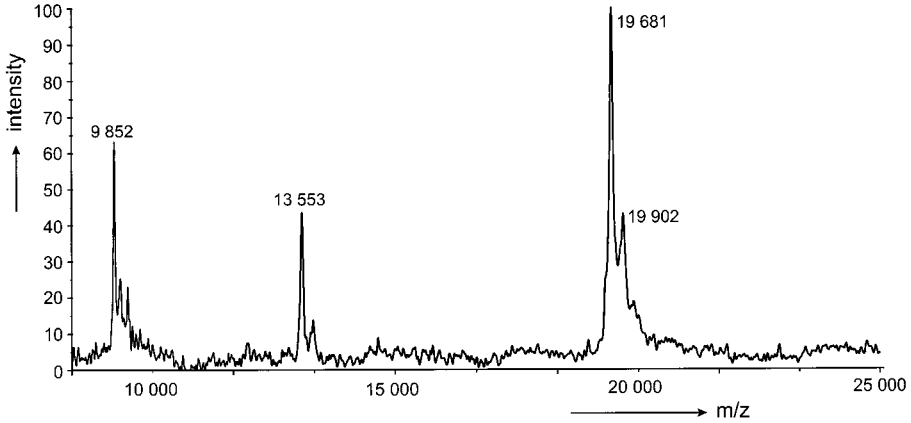

Figure 3. MALDI-TOF mass spectra of the monovalent Ag^+-complex of octarosette assemblies $\mathbf{1}_3$·$(EPB)_{24}$.

Conclusion

In summary, it can be stated that the quantitative self-assembly of 27 molecular components into one single nanostructure that is held together by a total of 144 hydrogen bonds adequately demonstrates the potential of molecular recognition as a tool to generate well-defined nanostructures via the bottom-up approach. More than this, we are able to control the dimensions of the assemblies in the range of 1−5 nm by a proper design of the calix[4]arene melamine component. Solid-phase synthesis could provide a means toward the synthesis of even higher generations of polymelamines. Our interest in these structures will mainly be directed toward their self-assembling behavior on flat surfaces, either via noncovalent interactions (rodlike structures)[6] or via covalent attachment to a flat surface (gold monolayers or colloids).

(13) Porath, D.; Bezryadin, A.; De Vries, S.; Dekker, C. *Nature (London)* **2000**, *403*, 635−637.

Experimental Section

General Methods. All experiments were performed in an inert atmosphere. THF was distilled from Na/benzophenone ketyl and CH_2Cl_2 from K_2CO_3. All chemicals were reagent grade and used without further purification. ^{1}H NMR spectra (300 MHz) were recorded in chloroform-d_1 or toluene-d_8. Samples for fast atom bombardment (FAB) mass spectrometry were loaded in a *m*-nitrobenzyl alcohol solution onto a stainless steel probe and bombarded with Xe atoms with a energy of 8 keV. Flash chromatography was performed on silica gel (SiO_2, E. Merck 0.040−0.063 mm, 230−240 mesh). Preparative TLC was performed using SiO_2 (1 mm). All commercially available reagents were used without further purification. The synthesis of dimelamine monocarbamate **2a**,[12] dimelamine diamine **2b**,[11] tetramelamine diamine **3a**,[12] and hexamelamine **4**[12] have been or will be described elsewhere.

Synthesis of Octamelamine 1. To a solution of mono-Boc-protected carbamate **2a** (141 mg, 0.101 mmol) and DIPEA (19 μL, 0.11 mmol) in CH_2Cl_2 (10 mL) was slowly added a solution of tetramelamine diamine **3a** (0.110 g, 50.8 μmol) in CH_2Cl_2

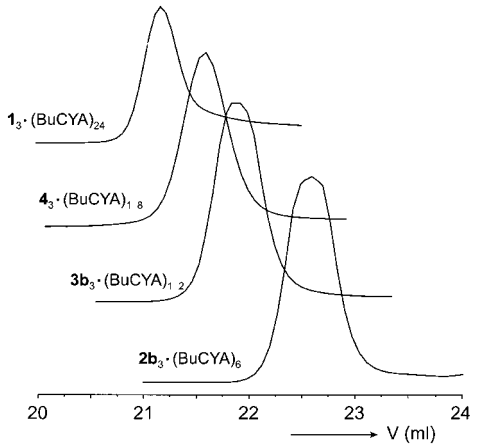

Figure 4. Gel permeation chromatography (GPC) data for octarosette assembly $\mathbf{1}_3$·(BuCYA)$_{24}$ in comparison to the double rosette assembly $\mathbf{2b}_3$·(BuCYA)$_6$. $CHCl_3$ was used as an eluent.

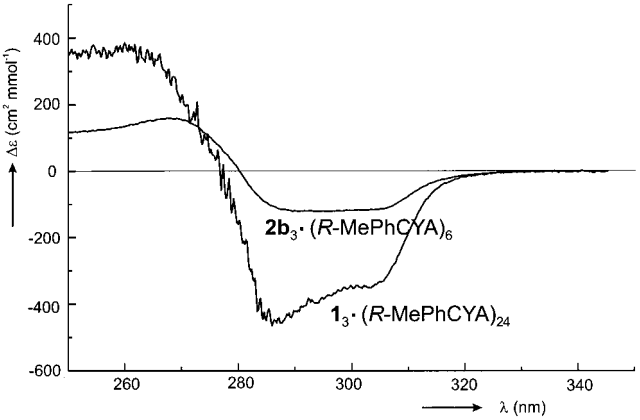

Figure 5. Circular Dichroism (CD) spectra of double rosette assembly $\mathbf{2b}_3$·(*R*-MePhCYA)$_6$ and $\mathbf{1}_3$·(*R*-MePhCYA)$_{24}$ in $CHCl_3$ (1.0 mM each).

(1 mL), and the reaction mixture was stirred for 2 h at rt. Then the reaction mixture was washed with H_2O (5 mL) and brine (5 mL) and dried over Na_2SO_4. After removal of the solvent under reduced pressure, the residue was purified by flash column chromatography (SiO_2, $CH_2Cl_2/CH_3OH-1\%$ NH_4OH, 90:10) giving pure **1** as an off-white solid in 31% yield (146 mg, 31 μmol). The ^{1}H NMR spectrum of free **1** shows mainly broad resonances, characteristic for self-aggregation of polymelamines: MS (FAB) m/z = 4665.4 (100, M^+, calcd 4665.8). Anal. Calcd for $C_{252}H_{352}N_{62}O_{26}$·$3CH_3OH$: C, 64.32; H, 7.70; N, 18.24. Found: C, 64.40; H, 7.65; N, 17.87.

Noncovalent Synthesis of Assemblies $\mathbf{1}_3$·(DEB)$_{24}$, $\mathbf{1}_3$·(BuCYA)$_{24}$, and $\mathbf{1}_3$·(*R*-MePhCYA)$_{24}$. The 27-component octarosette assembly $\mathbf{1}_3$·(DEB)$_{24}$ was prepared by mixing the octamelamine **1** with ~8 equiv of DEB in $CHCl_3$, followed by sonication and heating at 50 °C to ensure that assembly formation is under thermodynamic control: ^{1}H NMR δ 14.15 (s, 6H), 13.73, 13.71, 13.70 (3s, 18H), 13.30 (s, 6H), 12.96, 12.94, 12.90 (3s, 18H), 8.55, 8.50, 8.46 (3s, 18H), 8.28 (s, 6H), 7.7−7.4 (m, 24H), 7.05−6.2 (m, 144H), 5.97, 5.93 (2s, 24H), 5.2−5.0 (m, 48H), 4.5−4.2 (m, 48H), 4.0−3.6 (m, 96H), 3.6−3.4 (m, 48H), 3.2−2.2 (m, 60H), 2.2−1.4 (m, 228H), 1.4−0.6 (m, 486H): MALDI-TOF MS (after Ag^+-labeling) m/z = 19 681 (100, $[M+Ag]^+$, calcd for $C_{1044}H_{1344}N_{234}O_{150}$·$^{107}Ag^+$ = 19 679.2).

Octarosette assemblies $\mathbf{1}_3$·(BuCYA)$_{24}$ were prepared by addition of a slight excess (~26.4 equiv) of *N*-butylcyanuric acid (BuCYA) or *N*-(1*R*-phenylethyl)cyanuric acid (*R*-MePhCYA) to assembly $\mathbf{1}_3$·(DEB)$_{24}$, resulting in quantitative exchange of DEB with either BuCYA or chiral *R*-MePhCYA. The quantitative exchange of DEB for CYA was confirmed by ^{1}H NMR measurements (see Figure 2b), showing that the original signals for the assembly with DEB have completely disappeared.

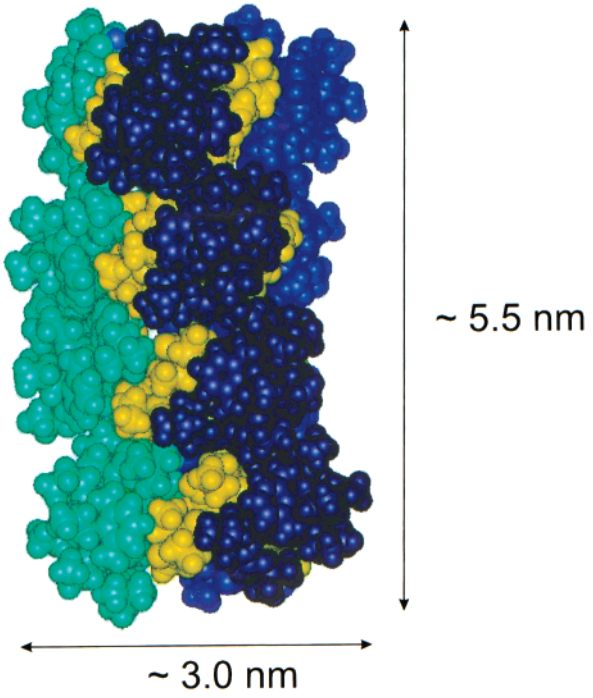

Figure 6. Computer-simulated structure (CHARMm 24.0) of octarosette assembly $\mathbf{1}_3$·(DEB)$_{24}$.

MALDI-TOF Mass Spectrometry[14] Measurements. For instrumentation and experimental conditions, see ref 7. Samples were prepared by mixing 10 μL of a 1 mM chloroform solution of the sample with 30 μL of a 0.01 mg/L solution of the matrix (= hydroxybenzylidene malononitrile) in chloroform/liquid poly(ethylene glycol) film. One microliter of this solution was loaded onto a gold-sample plate, coated with the prepared film, and transferred into the vacuum of the mass spectrometer for analysis.

GPC Measurements. GPC measurements were carried out at ambient temperature using a modular system comprising a Waters 510 pump, a HP1051-Ti autosampler, and a Waters 411 differential refractometer. All separations were obtained using three Waters columns(HR4 + HR2 + HR0) and one additional 500 Å guard column in series. As a solvent we used stabilized chloroform at a flow rate of 1.5 mL/min. The sample loading was 60 μL of a 0.05% w/v solution.

Molecular Mechanics Calculations. Initial structures as well as visualizations were generated using Quanta 97.[15] All gasphase simulations were performed with CHARMm version 24.0[16−18] as implemented in Quanta 97. Parameters were taken from Quanta 97 and point charges were assigned with the charge-template option. Residual charge was smoothed on carbon and nonpolar hydrogen atoms rendering overall neutral residues. A distance-dependent dielectric constant was applied with $\epsilon = 1$. No cutoffs on the nonbonded interactions were used. Energy minimizations were performed with the Steepest Descent and Adopted Basis Newton−Raphson methods until the root-mean-square of the energy gradient was <0.001 kcal mol^{-1} Å^{-1}.

JO0105742

(14) Karas, M.; Bachmann, D.; Bahr, U.; Hillenkamp, F. *Int. J. Mass Spectrom. Ion Processes* **1987**, *78*, 53−68.
(15) *Quanta 97*; Molecular Simulations: Waltham, MA.
(16) Brooks, B. R.; Bruccoleri, R. E.; Olafson, B. D.; States, D. J.; Swaminathan, S.; Karplus, M. *J. Comput. Chem.* **1983**, *4*, 187−217.
(17) Momany, F. A.; Klimkowski, V. J.; Schäfer, L. *J. Comput. Chem.* **1990**, *11*, 654−662.
(18) Momany, F. A.; Rone, R.; Kunz, H.; Frey, R. F.; Newton, S. Q.; Schäfer, L. *THEOCHEM* **1993**, *105*, 1−18.